



available at [www.sciencedirect.com](http://www.sciencedirect.com)



journal homepage: [www.elsevier.com/locate/psyneuen](http://www.elsevier.com/locate/psyneuen)



# Estrogen regulates cytoskeletal flexibility, cellular metabolism and synaptic proteins: A proteomic study

Éva M. Szegő<sup>a,b,c,\*</sup>, Katalin A. Kékesi<sup>a,d</sup>, Zoltán Szabó<sup>b</sup>,  
Tamás Janáky<sup>b</sup>, Gábor D. Juhász<sup>a</sup>

<sup>a</sup> Laboratory of Proteomics, Eötvös Loránd University, Budapest, Pázmány P. stny. 1/c, H-1117, Hungary

<sup>b</sup> Medical Chemistry Department, University of Szeged, Szeged, Dóm tér 8, H-6720, Hungary

<sup>c</sup> Department of Neurodegeneration and Restorative Research, Georg-August University, DFG Research Center: Molecular Physiology of the Brain (CMPB), Göttingen, Waldweg 33, D-37073, Germany

<sup>d</sup> Department of Physiology and Neurobiology, Eötvös Loránd University, Budapest, Pázmány P. stny. 1/c, H-1117, Hungary

Received 19 May 2009; received in revised form 3 November 2009; accepted 4 November 2009

## KEYWORDS

Cytoskeletal remodeling;  
*In vivo* microdialysis;  
Proteomics;  
Systems biology

**Summary** Estrogen (E2) influences brain function to induce gender differences in neuronal processes. In contrast to its well-described effects on signaling systems and gene transcription factors, our knowledge of E2-regulated protein networks is rather limited. Thus, we examined changes in protein expression patterns in the whole brains of ovariectomized mice after 24 h estrogen exposure using two-dimensional differential gel electrophoresis. Interpretation of our network-based hypothesis suggested that E2 regulates synaptic proteins and processes, increases cytoskeletal flexibility and alters glucose consumption in the brain. We verified the predicted reduced basal synaptic activity using *in vivo* microdialysis in conscious mice, showing that E2 decreases the extracellular concentrations of certain amino acids in two different brain areas (in the striatum and in the hypothalamus) and that this is independent from the E2 receptor densities. Our data reveal that E2 induces minor, but substantial changes to functionally different protein networks at the whole brain level, and as a cumulative effect, it adjusts the brain steady-state condition to a more flexible state.

Crown Copyright © 2009 Published by Elsevier Ltd. All rights reserved.

## 1. Introduction

17 $\beta$ -Estradiol (E2) engenders diverse effects in mammalian organisms, from those associated with its role as the main female sexual hormone to its controlling influence on tissue development, cell vulnerability, and incidence of neurodegenerative diseases (Bergemann and Riechter-Rössler, 2005). E2 and its receptors (estrogen receptor  $\alpha$ ,  $\beta$ , and X, ER $\alpha$ , ER $\beta$ , ERX) are present in most brain structures (Mitra et al., 2003; Merchenthaler et al., 2004). The cell protective effects of E2

\* Corresponding author at: Department of Neurodegeneration and Restorative Research, Georg-August University, DFG Research Center: Molecular Physiology of the Brain (CMPB), Göttingen, Waldweg 33, D-37073, Germany. Tel.: +49 551 3913547; fax: +49 551 3913541.  
E-mail address: [eszego@uni-goettingen.de](mailto:eszego@uni-goettingen.de) (E.M. Szegő).

in neurodegenerative disorders have been described previously (Garcia-Segura et al., 2001; Brann et al., 2007). In addition to the antioxidant effect observed at high concentration (Moosmann and Behl, 1999; Prokai et al., 2003), E2 also decreases cell vulnerability to various toxins and enhances repair after injury at a physiological level (Merchenthaler et al., 2003). E2 alters *de novo* synthesis of proteins involved in neuroprotective mechanisms, and decreases the concentrations of proteins responsible for over-excitation or sustained depolarization (Behl, 2002; Manthey and Behl, 2006; Zhou et al., 2007). It also regulates neuronal functions during puberty, lactation and menopause (Bergemann and Riechter-Rössler, 2005), and rapid changes in its level are frequently accompanied by mental or psychotic dysfunctions.

With receptor binding, E2 can alter gene transcription via direct insertion of ER–E2 complex into the DNA (classical effect) and also via activation of rapid signaling pathways and transcription factors (non-classical effect) (Kousteni et al., 2001; Revankar et al., 2005; Szegő et al., 2006). Several molecular mechanisms of E2 action are already known, and we have information about E2 regulation of certain genes and proteins, but our knowledge about the complexity and cooperativity of this regulation terminates at the level of transcription factors and gene transcription; effects on protein translation are as yet little explored. Connecting the physiologic roles of E2 to molecular events thus requires knowledge about E2-induced global protein expression alteration as only a very small fraction of transcribed genes are translated to proteins. As gene expression studies indicate that E2 induces transcription of large number of genes through estrogen response element (ERE) sites in the nervous system (Wang et al., 2004), the argument that E2 plays a role in shaping the proteome seems valid. Thus, several laboratories have examined the E2-induced proteome changes of the anterior pituitary (Blake et al., 2005) or the brain mitochondrial proteome (Nielsen et al., 2007). However, at the level of the whole brain, the main questions remain unsolved, namely which proteins are transcribed by E2-activated transcription factors and whether detectable protein changes can be linked to the biological functions of E2.

Two-dimensional differential gel electrophoresis (DIGE) was used to study changes in the protein composition of whole brain tissue after E2 treatment. Since we intended to search for complex and general mechanisms of E2-activated cell functions, a proteomic study on total brain tissue homogenate was performed to eliminate nervous tissue heterogeneity. On the other hand, using whole brain homogenizates resulted in the loss of regional differences. The transcriptional response after E2 exposure occurs in successive steps, and genes of the structural proteins are usually activated in the third or fourth steps, as a delayed response. As we wanted to address the protein expression pattern, which occurs hours after gene expression, 24 h seemed to be reasonable time to measure changes in the whole brain proteome caused by E2. After 24 h E2 exposure, we used DIGE and liquid chromatography-mass spectrometry (LC–MS) to separate and identify proteins with altered expression level. We identified 48 differently expressed protein spots, and then divided into seven functional groups, namely “Carbohydrate and fatty acid metabolism”, “Synaptic processes”, “Cytoskeleton”, “Protein metabolism”, “Signaling”, “Antioxidant mechanism” and “DNA/RNA processing”. We selected three proteins to

validate our proteomic results with Western blot and immunohistochemistry. Based on our proteomic results, we created networks of putative functional changes. As we hypothesized that E2 might modulate the excitatory neurotransmission and rearranges amino acid pools, we performed an *in vivo* microdialysis experiment to study the effect of E2 on extracellular amino acid (AA) levels in two different brain areas.

The major conclusions of our study are that E2 improves antioxidant mechanisms, modulates basal synaptic activity and enhances cytoskeletal flexibility, suggestive of a mechanism whereby brain cells under E2-stimulation are more capable of withstanding injury. The E2-induced fine tuning of multiple cellular systems, as evidenced by changes to the proteome, reveals a new view of an E2-induced molecular tuning within the central nervous system.

## 2. Materials and methods

### 2.1. Animals

Animal breeding and experiments were performed based on the rules of Local Animal Care Committee at the Eötvös Loránd University, in accordance with the European Union conforming Hungarian Act of Animal Care and Experimentation. Wild-type, C57BL6/J mice were maintained under a 12 h light/dark cycle at 20 °C, and they were supplied with water and food *ad libitum*.

### 2.2. Ovariectomy, tissue preparation

Adult female 45–60-day-old mice or 70–90-day-old mice (for microdialysis) were bilaterally ovariectomized (OVX) under deep anesthesia using Avertin (2% 2,2,2-tribromo-ethanol, 1,2% amyl-hydrate; 8% ethanol in physiological saline). On post-ovariectomy day 14, animals received a *subcutaneous* injection of 1 µg of 17β-estradiol (in 0.1 ml ethyl-oleate vehicle, Sigma, USA) or same amount of vehicle alone between 0800 h and 1000 h. Animals were sacrificed by cervical dislocation, brains were rapidly removed (<40 s) and frozen in dry ice. The cerebellum and the brainstem were removed and the forebrain was used for further analysis (henceforth called as whole brain or brain). Brains were stored at –80 °C until use in DIGE, Western blot or whole brain amino acid measurements. For immunohistochemical studies, mice were transcardially perfused with 4% paraformaldehyde (Merck, Germany; pH 7.6) in phosphate-buffered saline solution. Brains were postfixed for 2 h at 4 °C and cryoprotected in Tris-phosphate-buffered solution (TBS, pH 7.6) containing 30% sucrose overnight at 4 °C. 30 µm coronal sections were cut on a freezing microtome and four sets of sections were collected in TBS.

### 2.3. Protein isolation, DIGE and in-gel digestion

Brain tissue samples from vehicle ( $n = 6$ ) and E2-treated ( $n = 6$ ) mice were mechanically homogenized in an extraction buffer containing protease and phosphatase inhibitors (7 M urea, 2 M thiourea, 30 mM Tris, 20 mM magnesium acetate, 2% CHAPS; protease inhibitor mix (1:100, GE Healthcare, Uppsala, Sweden). After sonication (10 × 10 s), homogenates were centrifuged at 14,000 × g for 1 h at 4 °C. The pH of the supernatant was adjusted to 8.5 and protein concentrations

of the samples were determined by 2D-Quant Kit (GE Healthcare; protein content between 2 and 10  $\mu\text{g}/\mu\text{l}$ ). Samples of 50  $\mu\text{g}$  were labeled with CyDye DIGE Fluor Minimal Labeling Kit (GE Healthcare) at a concentration of 400 pmol/50  $\mu\text{g}$  protein. Samples (50–50  $\mu\text{g}$  from E2 or V treated mice, randomized groups, see Fig. 1A) were labeled with Cy3 or Cy5, the reference sample (internal standard, equal amounts: 25  $\mu\text{g}$  of all E2 and all V treated samples) was labeled with Cy2, and all three differently marked samples (50  $\mu\text{g}$  of E2, 50  $\mu\text{g}$  V and 50  $\mu\text{g}$  reference; Alban et al., 2003) were multiplexed to be resolved in the same gel (Fig. 1A). Labeled proteins were dissolved in isoelectric focusing (IEF) buffer containing ampholytes (0.5, v/v%), DTT (0.5, m/v%), 8 M urea, 30% glycerine, 2% CHAPS, and rehydrated passively onto 24 cm IPG strips (pH 3–10, GE Healthcare) for at least

14 h at room temperature. After rehydration, the IPG strips were subjected to first dimension IEF for 24 h to attain a total of 80 kVh. Focused proteins were first reduced by equilibrating with buffer containing 1% (w/v) mercaptoethanol for 20 min and then alkylated with a buffer containing 2.5% (w/v) iodoacetamide for 20 min. After reduction and alkylation, the IPG strips were loaded onto 10% polyacrylamide gels (24  $\times$  20 cm), and SDS-PAGE was conducted at 60 W for 6 h to resolve proteins in the second dimension. Following electrophoresis, gels were scanned in a TyphoonTRIO+ scanner (GE Healthcare) using appropriate lasers and filters with the PMT biased at 550 V. Images in different channels were overlaid using selected colors and differences were visualized using Image Quant software (GE Healthcare). Differential protein analysis was performed using DeCyder software package, DIA

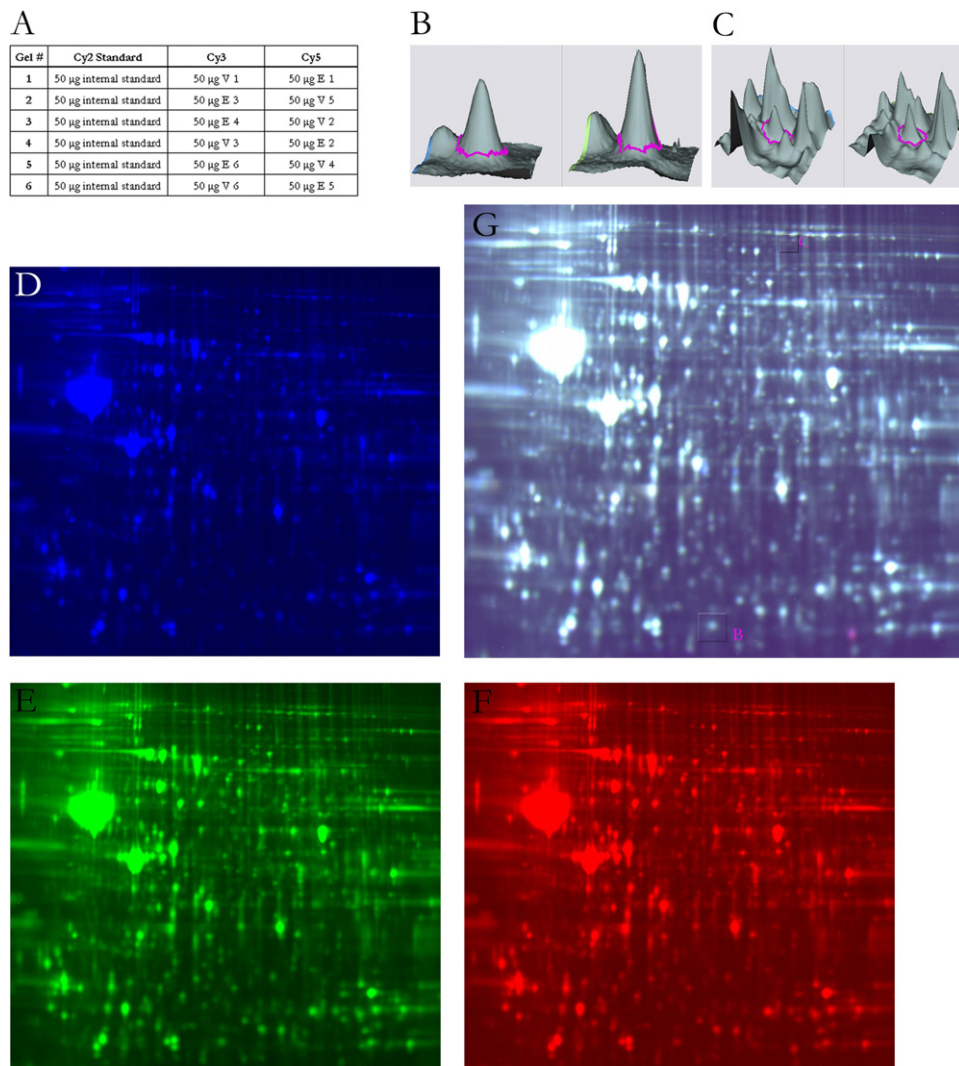


**Figure 1** Two-dimensional difference in-gel electrophoresis (DIGE) experimental design and representative gel maps. (A) Each gel was loaded with 50  $\mu\text{g}$  of Cy2-labeled protein pool from all samples as an internal standard (namely 5  $\mu\text{g}$  from each sample), 50  $\mu\text{g}$  of Cy3-labeled and 50  $\mu\text{g}$  of Cy5-labeled sample as indicated (see Section 2). V: 0.1 ml ethyl-oleate (vehicle); 24 h, E2: 1  $\mu\text{g}$  17 $\beta$ -E2 in 0.1 ml vehicle, 24 h. (B, C) three-dimensional images from significantly altered spots, as visualized by BVA module of DeCyder software. The positions of the proteins on DIGE gel are showed in G. (D–G) Representative DIGE images. Proteins were extracted from total brain homogenizates of mice 24 h after they received a single injection of E2 or vehicle. Proteins were labeled with one of the CyDyes (D: Cy2, E: Cy3, F: Cy5, G: merged; see panel A). Proteins were separated on 24 cm pH 3–10 nonlinear strips (isoelectric focusing) followed by the 10% SDS-PAGE. Gels were scanned with a Typhoon TRIO+ variable mood fluorescent scanner.

and Biological Variance Analysis (BVA) modules (GE Healthcare). For the identification of proteins in spots of interest, preparative 2D electrophoresis was performed separately using a total of 800 µg of proteins per gel. Resolved protein spots were visualized by Colloidal Coomassie Blue G-250 staining protocol. Four preparative gels were run, and 75 spots were picked for protein identification. Individual spots were excised from the gel, destained, and subjected to in-gel digestion with trypsin for 24 h at 37 °C (modified from Shevchenko et al., 1996). Tryptic peptides, extracted from gel pieces using 5% formic acid, were dried under vacuum.

#### 2.4. LC–MS analysis and protein identification

All LC–MS experiments were performed using Agilent 1100 Series nano-LC coupled through an orthogonal nanospray ion source to an Agilent LC-MSD XCT Plus ion trap mass spectrometer (Agilent Co., USA). The nano-LC system was operated in sample enrichment/desalting mode using a ZORBAX 300SB-C18 enrichment column (0.3 × 50 mm, 5 µm), and for chromatography we used ZORBAX 300 SB-C18 (75 µm × 150 mm) nanocolumn. Elution of peptides was accomplished by gradient elution at a flow rate of 300 nL/min using solvent A (0.1% formic acid in water) and solvent B (0.1% formic acid in acetonitrile) with a gradient from 100% solvent A to 40% solvent B in 40 min. MS was operated in peptide scan auto-MS/MS mode, acquiring full-scan MS spectra (300–1600 *m/z*) at a scan speed of 8100 um/s and a resolution of less than 0.35 um (FWHM). From the four most abundant peaks in the MS spectrum, automated, data-dependent MS/MS was used to collect MS/MS spectra (100–1800 *m/z* at 26,000 um/s and a resolution of less than 0.6 um, FWHM). All acquired data were processed and peaklists were generated by the Agilent DataAnalysis 3.2 software using default settings. Proteins were identified by database search using Mascot 2.2.04 (Matrix Science Inc. London, UK) against the NCBI database (2008.07.18 version, containing 6,833,826 entries) using a fragment ion mass tolerance of 0.80 Da and a parent ion tolerance of 1.5 Da. Carboxyamidomethylation of Cys and oxidation of Met were specified as variable modifications, and one trypsin missed cleavage was allowed. For all protein assignments, a minimum of two significant unique peptides were required, peptide assignments below significance threshold were manually validated to be included in sequence coverage calculation.

#### 2.5. *In vivo* microdialysis in freely moving mice

We used bilaterally ovariectomized, 70–90-day-old mice (*n* = 5/group) for these experiments. Under deep anesthesia (1.5% halothane in air, 1.8 l/min flow rate) mice were placed into a stereotaxic device equipped with dual manipulator arms and an anesthetic mask (Supertech, Pécs, Hungary). Microdialysis probes, made of hollow fibers (Travenol, cutoff: 5000 Da, od: 0.2 mm) were implanted into the right caudate putamen (CPu, AP: 0.9, L: –2.0, DV: –2.0) and into the left hypothalamus (HT, AP: –0.35, L: 0.5, DV: –5.0). The active surfaces of the probes were adjusted to the brain area: 2 mm for CPu, 1 mm for HT. After implantation, probes were glued to the skull, and mice were allowed to recover from surgery for at least 2 h. We limited our experimental procedure to 3–27 h

after probe insertion, allowing enough time after the initial injury for the blood–brain barrier to exclude large molecules but terminating the experiment before gliosis could develop. During surgery and sample collection, probes were perfused with non-pyrogenic, AA-free artificial cerebrospinal fluid (in mM: 144 NaCl, 3 KCl, 1 MgCl<sub>2</sub> and 2 CaCl<sub>2</sub>, pH 7.3, flow rate: 0.5–1 µl/min). Each experiment started with collection of three to four control samples (30 min each). Five hours after surgery mice received 1 µg 17β-estradiol (in 0.1 ml ethyl-oleate vehicle) or vehicle *subcutaneously*, then three to four samples were collected (30 min) (flow rate was adjusted to 0.1 µl/min for overnight). Next day the flow rate was set to 1 µl/min for at least 3 h before sampling and 22–24 h after E2 treatment samples were collected and kept on –20 °C until chromatography measurements.

For full scale tissue AA measurements, mice were decapitated 24 h after E2 or vehicle treatment. Brains were rapidly removed and irradiated in a microwave oven (800 W, 5 s). Whole brains without the cerebellum (*n* = 6/group) or HT and striata (*n* = 6/group) were used. Tissues were mechanically homogenized in solution B (50 µl/mg wt tissues, see later), centrifugated (30 min, 14,000 × *g*) and stored at –20 °C until AA measurements.

#### 2.6. Extended literature search: finding connections between altered proteins

To make a functional interpretation of our data, we performed an extended literature search to create protein interaction networks relating to the molecular mechanism of E2 action. The EXPASY Proteomics Server (<http://www.expasy.ch>, Swiss Institute of Bioinformatics, Switzerland), the electronic U.S. National Library of Medicine at the National Institutes of Health (<http://www.ncbi.nlm.nih.gov>, MD, USA) and the Google Toolbar (<http://www.google.com>, Google Inc., CA, USA) were used as databases.

#### 2.7. Measurement of the concentration of amino acids

Concentrations of AAs (glutamate: Glu, glutamine: Gln, aspartate: Asn, asparagine: Asn, GABA, glycine: Gly, serine: Ser, threonine: Thr, arginine: Arg, alanine: Ala) were measured by precolumn derivatization of primary AAs with orthophthalaldehyde (OPA). The derivatization reaction was performed at pH 10.4 in the presence of mercaptoethanol. OPA derivatized AAs were detected using 340 nm excitation and 440 nm emission wavelength of a fluorescent detector. Because of the instability of OPA derivatives, the HPLC technique was automatized on a HP 1100 series system. AAs were separated by HP Hypersyl ODS reversed phase columns (200 × 2.1 mm), filled with 5 µm C-18 spherical packing material. Eluent A was 0.1 M phosphate buffer containing 0.5% tetrahydrofuran, pH 6.0, eluent B contained 70% acetonitrile in eluent A, pH 6.0. The gradient profile was: 12% B at 0 min, 23% B at 9 min, 36% B at 18 min, 100% B at 20 min, 100% B at 25 min and 12% B at 28 min. The column equilibration time was 8 min. External standards of 10 µM AAs were injected after every 20 samples. Chromatograms were evaluated by HP ChemStation software (HP Hungary).

## 2.8. Immunohistochemistry

Free-floating, double-labeling, peroxidase based immunohistochemistry was performed in the same manner we reported previously with only a slight modification (Szegő et al., 2006; number of animals:  $n = 5$ /group). In brief, every fourth section was incubated with one of the primary antibodies (Calpain 1, 1:1000, Abcam, Cambridge, UK; Superoxide Dismutase 2

(SOD2), 1:2000, Abcam; Coronin 1B, 1:500, Santa Cruz Biotechnology, CA, USA) for 48 h at 4 °C. We selected the proteins based on the following criteria: (1) Different “functions”: calpain contributes to “protein metabolism”, “synapse” and “cytoskeleton”, coronin associated with “cytoskeleton”, SOD2 is a member of “antioxidant network” (see Table 1); (2) direction of change: calpain and SOD2 increased and coronin decreased after E2 treatment; and (3) commercially available

**Table 1** Proteins altered after 24 h E2 treatment, as identified using DIGE and peptide mass fingerprinting. Expression of proteins decreased after E2 treatment is shown in blue. Fold change: ratios of protein expression levels were calculated using DeCyder software package, Biological Variance Analysis module, as the fold change between normalized spot volume of vehicle and E2-treated samples. Values below zero: decreased protein level after 24 h E2 treatment. MW: molecular weight; pI: isoelectrical point; MW and pI as determined by Uniprot database; % Seq: protein sequence coverage by peptide mass fingerprinting.

|  | Spot No. | Acc. No.   | Protein name  | p-value                            | Fold change | MW     | pI    | % Seq | Subcellular localization |           |
|--|----------|------------|---|------------------------------------|-------------|--------|-------|-------|--------------------------|-----------|
| Cytoskeletal                           | 2668     | NP_062692  | ADP-ribosylation factor-like 3                          | 0.0025                             | 1.23        | 20645  | 6.74  | 37    | cytoplasm                |           |
|  | 1371     | NP_034028  | coronin, actin binding protein 1A                       | 0.043                              | -1.39       | 51641  | 6.05  | 10    | cytoplasm                |           |
|  | 2771     | NP_083085  | actin related protein 2/3 complex/ subunit 5-like       | 0.041                              | 1.29        | 17027  | 6.32  | 22    | cytoplasm                |           |
|  | 682      | BAC65593   | mKIAA0567 protein                                       | 0.023                              | -1.24       | 110852 | 7     | 5.3   | mitochondria             |           |
|  | 982      | BAC41423   | mKIAA0417 protein                                       | 0.024                              | 1.16        | 75687  | 6.56  | 16    | cytoplasm                |           |
|  | 1789     | AAH14867   | Protein phosphatase methyltransferase 1                 | 0.045                              | -1.19       | 42628  | 5.67  | 16    | cytoplasm                |           |
|  | 2612     | AAH55338   | Transgelin-3, Neuronal protein NP25                     | 0.021                              | 1.21        | 24981  | 6.53  | 39    | cytoplasm                |           |
|  | 1446     | AAH37137   | Fscn1 protein   | 0.023                              | -1.12       | 52157  | 6.57  | 24    | cytoplasm                |           |
|  | 2101     | AAC52639   | LASP1   | 0.041                              | 1.33        | 23087  | 5.11  | 42    | cytoplasm                |           |
|  | Synaptic | 544        | AAA37318  | dynamitin                          | 0.025       | -1.15  | 96209 | 6.32  | 10                       | cytoplasm |
|  |          | 642        | CAM15857  | dynamitin 1                        | 0.034       | -1.13  | 97925 | 6.59  | 27                       | cytoplasm |
| 681                                    |          | CAA38397   | D100  | 0.021                              | -1.18       | 96209  | 6.32  | 5     | cytoplasm                |           |
| 898                                    |          | P46460     | Vesicle-fusing ATPase (Vesicular-fusion protein NSF)    | 0.036                              | -1.32       | 83083  | 6.52  | 11    | cytoplasm                |           |
| 1134                                   |          | NP_035321  | synaptotagmin binding protein 1                         | 0.034                              | -1.24       | 68058  | 6.62  | 30    | cytoplasm                |           |
| 1325                                   |          | NP_032939  | protein phosphatase 3, catalytic subunit, alpha isoform | 0.0045                             | -1.48       | 59291  | 5.58  | 13    | nucleus, cytoplasm       |           |
| 1426                                   |          | NP_031535  | vacuolar H+ATPase B2                                    | 0.019                              | -1.37       | 56857  | 5.57  | 44    | vesicle, raft            |           |
| 1661                                   |          | AAK71661   | oxysterol-binding protein-related protein-1             | 0.035                              | -1.15       | 50512  | 6.62  | 15    | cytoplasm                |           |
| 2206                                   |          | NP_062606  | N-ethylmaleimide sensitive fusion protein attachment B  | 0.029                              | 1.38        | 33878  | 5.32  | 7     | cytoplasm                |           |
| 1473                                   |          | NP_036702  | glutamate dehydrogenase 1                               | 0.031                              | -1.07       | 61719  | 8.05  | 31    | mitochondria             |           |
| 1893                                   |          | NP_034455  | glutamate oxaloacetate transaminase 2, mitochondrial    | 0.012                              | 1.16        | 47780  | 9.13  | 37    | mitochondria             |           |
| 1712                                   |          | NP_032157  | glutamin synthetase                                     | 0.011                              | -1.17       | 42834  | 6.64  | 13    | cytoplasm                |           |
| Carbohydrate and fatty acid metabolism |          | 1043       | BAC28685  | glycerol phosphate dehydrogenase 1 | 0.016       | -1.3   | 81345 | 6.17  | 44                       | cytoplasm |
|  | 1438     | NP_033786  | aldehyde dehydrogenase 2                                | 0.00089                            | -1.13       | 57015  | 7.53  | 6     | mitochondria             |           |
|  | 1792     | AAI08373   | phosphoglycerate kinase 1                               | 0.018                              | -1.09       | 30124  | 8.96  | 11    | cytoplasm                |           |
|  | 1734     | AAH13554   | citrate synthase  | 0.031                              | -1.24       | 51988  | 8.72  | 16    | mitochondria             |           |
|  | 1738     | AAH03898   | Ndufs2 protein  | 0.00052                            | -1.42       | 53697  | 6.43  | 14    | mitochondria             |           |
|  | 2142     | NP_077183  | pyruvate dehydrogenase (lipoamide) beta                 | 0.009                              | -1.14       | 39254  | 6.41  | 33    | mitochondria             |           |
|  | 2351     | AAA37357   | CAH2  | 0.02                               | -1.24       | 29165  | 6.49  | 7     | cytoplasm                |           |
|  | 2354     | AAC37635   | Purine nucleoside phosphorylase                         | 0.02                               | 1.17        | 32538  | 5.93  | 7     | nucleus, cytoplasm       |           |
|  | 2474     | NP_1080971 | electron transferring flavoprotein beta-polypeptide     | 0.008                              | 1.23        | 27834  | 8.24  | 10    | mitochondria             |           |
|  | 2600     | AAH21616   | NADH dehydrogenase (ubiquinone) Fe-S protein 8          | 0.0088                             | 1.12        | 24452  | 5.89  | 26    | mitochondria             |           |
|  | 2631     | CAB52407   | Adenylate kinase  | 0.014                              | 1.15        | 21640  | 5.67  | 49    | cytoplasm, mitochondria  |           |
|  | 1204     | NP_034085  | dihydropyrimidinase-like 2                              | 0.047                              | -1.11       | 62638  | 5.95  | 66    | cytoplasm                |           |
|  | 1262     | NP_001378  | dihydropyrimidinase-like 3                              | 0.011                              | 1.32        | 62323  | 6.04  | 18    | cytoplasm                |           |
|  | 2570     | NP_033822  | apolipoprotein A-I                                      | 0.003                              | 1.11        | 30597  | 5.51  | 36    | secreted                 |           |
| Protein metabolism                     | 1501     | NP_035840  | tryptophanyl-tRNA synthetase                            | 0.049                              | -1.15       | 54861  | 6.44  | 24    | cytoplasm, mitochondria  |           |
|  | 1304     | BAA93551   | deubiquitinating enzyme                                 | 0.036                              | 1.13        | 56424  | 5.2   | 20    | cytoplasm                |           |
|  | 1577     | Q9Z2WO     | Aspartyl aminopeptidase                                 | 0.041                              | 1.38        | 52704  | 6.66  | 9     | cytoplasm                |           |
|  | 2485     | AAH08222   | Proteasome (prosome, macropain) subunit, alpha type 7   | 0.032                              | 1.21        | 28009  | 8.59  | 11    | cytoplasm                |           |
|  | 2488     | NP_033925  | Calpain, small subunit 1                                | 0.004                              | 1.18        | 28559  | 5.41  | 7     | cytoplasm                |           |
| DNA/RNA                                | 1865     | NP_058580  | heterogeneous nuclear ribonucleoprotein C               | 0.012                              | 1.12        | 34421  | 4.92  | 7     | nucleus                  |           |
|  | 1918     | AAH04706   | Hnrpc protein   | 0.049                              | 1.27        | 32257  | 5.01  | 13    | nucleus                  |           |
|  | 1968     | NP_035351  | purine rich element binding protein B                   | 0.049                              | 1.32        | 33995  | 5.35  | 20    | nucleus                  |           |
| Signaling                              | 1133     | NP_035845  | WD repeat domain 1                                      | 0.033                              | -1.09       | 67049  | 6.11  | 13    | nucleus, cytoplasm       |           |
|  | 2213     | NP_032876  | phosphatidylinositol transfer protein, alpha            | 0.0095                             | -1.13       | 32101  | 5.97  | 24    | nucleus, cytoplasm       |           |
| Antioxidant                            | 2518     | NP_034488  | glutathione S-transferase, mu 1                         | 0.012                              | 1.18        | 26067  | 7.71  | 13    | cytoplasm                |           |
|  | 2592     | AAH05626   | Peroxiredoxin 3   | 0.041                              | 1.32        | 28337  | 7.15  | 10    | mitochondria             |           |
|  | 2670     | CAA28645   | manganese superoxide dismutase                          | 0.039                              | 1.21        | 24890  | 8.8   | 36    | mitochondria             |           |

antibody can be used both for Western blot and immunohistochemistry. After incubation with the primary antibodies, sections were incubated with biotinylated IgG (1:200; Vector Laboratories, Burlingame, CA, USA) for 2 h, followed by treatment with Vector avidin–biotin–horseradish peroxidase (HRP) complex (Vector Standard Elite Kit, 1:200) for 2 h. Peroxidase labeling was visualized by nickel-diaminobenzidine tetrahydrochloride. The omission of primary antibodies resulted in a complete absence of immunoreactivity (ir).

## 2.9. Western blot

Frozen brain samples ( $n = 5–6$ /group) were homogenized in lysis buffer containing 20 mM Tris, 1 mM EDTA, 100 mM NaCl in the presence of protease and phosphatase inhibitors (Protease Inhibitor Mix, 1:100, GE Healthcare; Apronitin, 0.4  $\mu$ M, Phenylmethanesulfonyl fluoride, 2 mM, Sodium orthovanadate, 2 mM, Leupeptin, 10  $\mu$ M, Sigma). After sonication and centrifugation (4 °C, 9500  $\times$  g, 30 min) cytoplasm and membrane fractions (25  $\mu$ g) were resolved on a 10% polyacrylamide gel. Proteins were transferred onto a nitrocellulose membrane (Bio-Rad, USA). We cut the membrane into three pieces (by the MW of the proteins: calpain: 75 kDa, coronin: 57 kDa, SOD2: 25 kDa), then pieces of membranes were blocked in 5% nonfat milk in Tris–Tween buffer (500 mM Tris, 150 mM sodium chloride, pH 7.4, and 0.05% Tween 20 (Sigma) for coronin and SOD2 or in 5% gelatine (Merck) for calpain for 1 h, incubated with polyclonal anti-coronin 1B, anti-SOD2 (1:3000) or anti-calpain (1:2000) (1:500) antibodies in Tris–Tween buffer for 24 h at 4 °C. After incubation with HRP-conjugated secondary antibody (1:2000, Santa Cruz), bands were visualized using SuperSignal West Pico Chemiluminescent Substrate (Pierce, IL, USA).  $\beta$ -Actin protein abundance was used as control for equal protein loading and transfer (anti- $\beta$ -actin antibody, 1:2000, Sigma, visualized in the piece of membrane).

## 2.10. Data analysis and statistics

For DIGE experiments, statistics were calculated by the DeCyder software (GE Healthcare), Biological Variance module. The  $p$  values ( $t$ -test) were determined for each protein spot. The internal standard was a pool of equal amounts of all samples within the experiment, and it was representative of every protein present and was the same across all gels. The standard provided an average image against which all other gel images were normalized, thus removing much of the experimental variation and reducing gel-to-gel variation. Determination of the relative abundance of the fluorescent signal between the internal standards across all gels therefore provided standardization between all gels. Data on AA measurements are expressed as percentage of control values  $\pm$  SEM. Data on results of Western blot experiments were expressed as mean of optical densities (normalized for actin and then to vehicle-treated controls)  $\pm$  SEM. Alterations of extracellular levels of AAs and optical densities of Western blots were evaluated by one-way analysis of variance (ANOVA, Statistica 7.0, StatSoft, Tulsa, OK, USA) followed by Newman–Keuls *post hoc* test. A  $p$  level of 0.05 was taken as indicative of statistical significance of tests. Number of calpain, SOD2 or coronin ir cells were counted by an Olympus BX51 (Olympus

Optical, Hamburg, Germany) microscope, using 20 $\times$  and 40 $\times$  objectives. Structures to be analyzed were selected based on the average estrogen receptor contents (Paxinos and Franklin, 2001; Mitra et al., 2003; Merchenthaler et al., 2004). The following structures were selected: mainly ER $\alpha$ -containing areas: lateral septum, hippocampus (CA1–3); mainly ER $\beta$ -containing areas: medial septum, piriform cortex; areas abundant in both types of receptors: amygdala, paraventricular nucleus, anterior HT; areas at low level of receptors: somatosensory cortex, striatum. Every fourth section was stained with the corresponding antibody, three sections from each structure were selected and an investigator blind to the experimental grouping determined the numbers of ir cells. We used AnalySYSPro software (Olympus Ltd., Budapest, Hungary) for cell counting; areas of interest were adjusted to the given region. The number of neurons/ $\mu$ m<sup>3</sup> was determined. Data are expressed as mean  $\pm$  SEM. To examine the differences between vehicle and E2-treated animals, Mann–Whitney  $U$  test was used (Statistica).

## 3. Results

### 3.1. Identification of differentially expressed protein spots

The DIGE method allowed us to separate and visualize approximately 1500–3000 protein spots per gel. From a 3  $\times$  50  $\mu$ g sample, a total of 3120 spots were present on the master gel, as determined using DeCyder software (GE Healthcare, Uppsala, Sweden). The experimental design allowed direct comparison between vehicle-treated or E2-treated animals and the internal standard. The reliability of the experimental groups was verified by the fact that E2 administration or ovariectomy effectively altered the plasma E2 concentration (Szegő et al., 2006). After 24 h E2 treatment, the majority of protein spots showed only small changes between groups, but the intensity of 75 spots were found, using standard  $t$ -test across all gels ( $n = 6$ ), to show a statistically significant difference. From these 75 spots, 34 showed increased expression after E2 exposure, while 41 spots decreased in expression, relative to the internal standard. A representative 2D gel and significantly altered spots are shown in Fig. 1. Because of small amount of CyDye-labeled proteins in one spot, we cast “preparative” gels (800  $\mu$ g protein/gel) stained with Colloidal Coomassie Blue G-250 for MS identifications. Protein patterns of CyDye-labeled and Coomassie-stained gels were identical and all spots of interest matched well and could be picked out. Identifications were made from peptide mass fingerprint followed by database search. Out of 75 spots of interest, we were able to identify 48 spots based on the criteria of successful match. Identified proteins, showing significant differences, are listed in Table 1.

The identified proteins could be classified into seven groups according to their biological functions: “Carbohydrate and fatty acid metabolism” (14 identified protein spots), “Synaptic processes” (12), “Cytoskeleton” (9), “Protein metabolism” (5), “Signaling” (2), “Antioxidant mechanism” (3) and “DNA/RNA processing” (3). The majority of the identified changes occurred in proteins that regulate the cytoskeleton or cellular energetics. Cytoskeletal

proteins that were increased regulate the post-translational modification of tubulin and branching of the actin filament (ADP-ribosylation factor-like 3, coronin, actin related protein 2/3 complex, protein phosphatase methylesterase 1 or fascin). Enzymes related to the glucose metabolism were decreased (including glycerol phosphate dehydrogenase 1, phosphoglycerate kinase 1, pyruvate dehydrogenase (lipoamide) beta and citrate synthase). On the other hand, members of the electron transport chain were increased by E2 treatment (ubiquinone Fe-S 8, electron transferring flavo-protein beta-polypeptide). Synapse-related proteins were also found to be changed after E2 treatment (including: vesicular-fusion protein, syntaxin binding protein 1, N-ethylmaleimide sensitive fusion protein attachment B and dynamin). Among the proteins regulating the oxidative balance of the cells, peroxiredoxin 3, glutathione S-transferase and manganese superoxide dismutase were increased after E2 injection. We also identified proteins involved in the regulation of translation, the heterogeneous nuclear ribonucleo-protein C and purine rich element binding protein B. Both proteins were increased after exposure to E2.

### 3.2. Confirmation of DIGE results with Western blot and immunohistochemistry

We selected three of the identified proteins to validate our proteomic results with Western blot and immunohistochemistry. Expression of calpain 1 (“Protein metabolism”, “Cytos-

keletal”) and SOD2 (“Antioxidant”) were increased, while coronin 1 (“Cytoskeletal”) decreased after E2 treatment, according to our DIGE results. Although the Western blot method can only detect large changes in protein concentrations comparing to DIGE, the level of SOD2 and calpain were increased significantly in whole brain preparations ( $p = 0.0179$  for SOD2 and  $p = 0.0304$  for calpain; Fig. 2A, B). We also detected a small, non-significant decrease in coronin expression ( $p = 0.2545$ ).

We analyzed the regional distributions of the three selected proteins using immunohistochemistry. Numbers of immunoreactive (ir) cells showed no change following E2 treatment in any of the brain areas investigated (Fig. 2C), and the location of the ir-signal did not correlate with the known distribution of ERs.

### 3.3. E2 reduces extracellular concentrations of amino acids

One of our hypotheses was that E2 treatment influences the basal synaptic processes and protein metabolism and thus, E2 should alter the amino acid concentration in the extracellular space. To address this question, we used microdialysis in conscious, freely moving mice. The microdialysis probes were implanted into the right caudate putamen (low density of classical ERs) and into the left HT (high density of classical ERs) of mice (Mitra et al., 2003; Merchenthaler et al., 2004). After 24 h, injection of 1  $\mu\text{g}$  17 $\beta$ -estradiol induced a significant

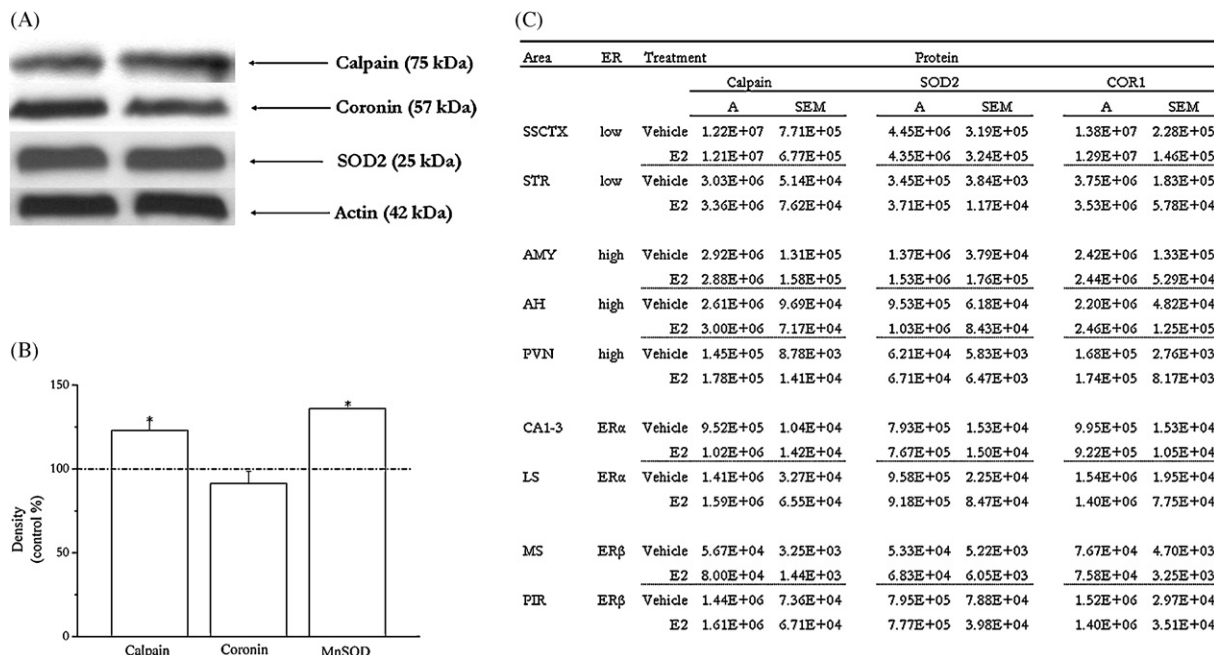


**Figure 2** Western blot and immunohistochemical validation of calpain, coronin and SOD2 expression. (A) Calpain, coronin, SOD2 and the endogenous reference protein actin were simultaneously detected in samples of control (V) and E2-treated (E2) mice after SDS-PAGE and electroblotting into nitrocellulose membrane. (B) Expression of calpain and SOD2 were significantly higher after 24 h E2 treatment, while coronin did not change. Data are expressed as mean  $\pm$  SEM, in control %. (C) 24 h treatment with E2 had no effect on the number of calpain, SOD2 or coronin-immunoreactive cells in areas with different estrogen receptor expressions. Numbers of immunoreactive cells are expressed as mean  $\pm$  SEM. SOD2: superoxide dismutase 2; SSCTX: somatosensory cortex; STR: striatum; AMY: amygdala; AH: anterior hypothalamus; PVN: paraventricular nucleus; CA1–3: hippocampus, CA1–3 regions; LS: lateral septum; MS: medial septum; PIR: piriform cortex; ER: estrogen receptor; A: average cell number; low/high: areas with low/high average estrogen receptor content (both type); and ER $\alpha$  or ER $\beta$ : areas containing mainly ER $\alpha$ /ER $\beta$ -expressing cells.

decrease in the extracellular concentrations of certain AAs measured from the dialyzates (Fig. 3). On the other hand, we observed decreased level of Asp and Gln from tissue homogenizates of STR and HT. Decrease of Asp and Gln was accompanied by decrease of GABA, Glu and Ser in the STR. In the HT, decreased level of Asn, Arg and Ala was detected together with Asp and Gln. E2 treatment did not induce changes in the concentrations of AAs at the level of the total brain (Fig. 3).

#### 4. Discussion

In the present study, adult ovariectomized mice were treated with E2, which induced substantial changes in the whole brain proteome within 24 h. These changes suggest that E2 induces functional alterations to cytoskeletal dynamic flexibility, basal synaptic activity, ATP production, antioxidant mechanisms and protein metabolism. Changes in the expres-

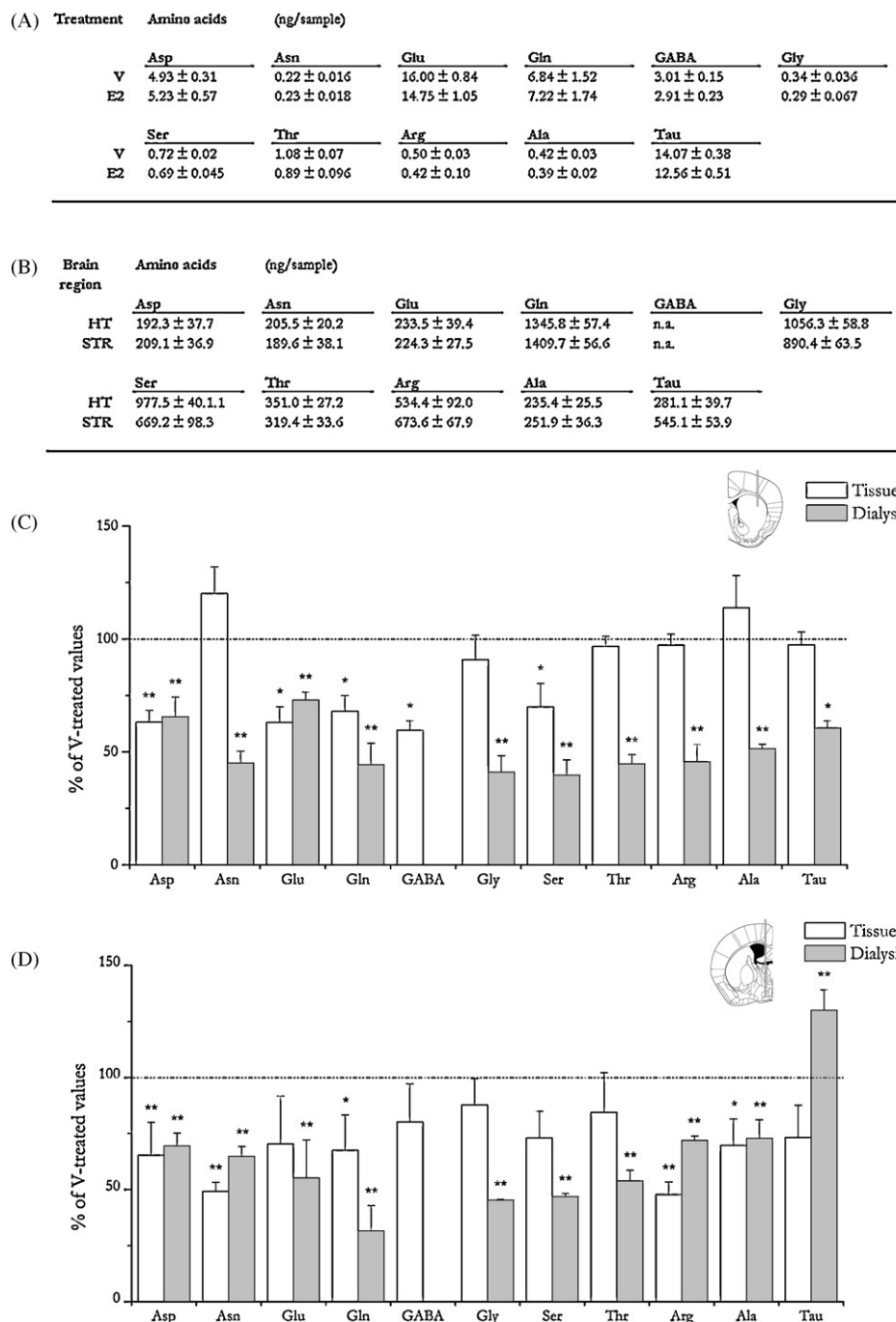


**Figure 3** E2 decreases the extracellular concentration of excitotoxic amino acids. (A) 24 h E2 treatment did not induce any changes in the concentrations of total brain amino acids. V: vehicle, 24 h; E2: 1 µg 17β-E2 in 0.1 ml vehicle, 24 h. Data are expressed as mean ± SEM. (B) Resting amino acid levels in the microdialysates from the hypothalamus (HT) or from the striatum (STR) of freely moving mice. Data are expressed as mean ± SEM. (C, D) Changes in tissue and extracellular concentrations of certain amino acids after E2 or V treatment in the striatum (C) and in the hypothalamus (D). Inserts show the place of microdialysis probes (Paxinos and Franklin, 2001). Data are expressed as mean ± SEM ( $n = 5-6$ /group; \*:  $p < 0.05$ , \*\*:  $p < 0.01$ ; n.a.: not available), in the % of control (V) samples.

sion level of a relatively high number of cytoskeletal and metabolic proteins show that a considerable part of the cellular protein network responded to E2. Because of the limitations of protein identification, proteomics data must be validated using independent methods. However, due to the large number of hits, validation of all proteomic results could not be accomplished. We therefore selected three proteins from different functional protein networks, SOD2, coronin and calpain, for Western blot analysis and immunohistochemical studies. Western blot results confirmed the significant increase in SOD2 and calpain levels, but the decrease of coronin was under the level of significance. The number of immunoreactive cells did not change, indicating that cells already expressing SOD2 or calpain increased the protein expression as a response to E2. In addition, one of the important brain functions altered by E2 was synaptic transmission. Because extracellular AA levels sensitively reflect the amount of transmitters released at the synapse, cellular metabolism and energy production, we measured AA changes in the brain extracellular space and in the tissue. Our results show that E2 reduces the extracellular AA concentration in the hypothalamus and in the striatum, evidence of E2's role in modulating synaptic transmission. Thus, Western blotting, immunohistochemistry and microdialysis studies together confirm the validity of our proteomics results.

#### 4.1. Putative functional protein pathways influenced by E2

A major problem in discussion of proteomic results is how to develop functional hypotheses based on the protein changes measured. Generating mere lists of proteins provides limited

biological information. In order to come to a better understanding of cellular function, data interpretation must additionally include a thorough literature search. Thus, we tried to construct protein networks based on hypotheses concerning E2-activated functional changes, including regulation of the cytoskeleton (Fig. 4), metabolism and synaptic silencing, which we describe in detail below. Hereafter the names of proteins with altered expression are in bold, see Table 1.

##### 4.1.1. Estrogen increases cytoskeletal flexibility

The small G protein **ADP-ribosylation factor-like 3** (Arl3) is important in tubulin deacetylation, membrane trafficking and in lipid metabolism. The majority of the  $\alpha$ -tubulin content is acetylated in cells, and the polymer becomes destabilized after losing the acetyl-group (Black et al., 1989). The  $Ca^{2+}$ -activated cysteine-protease, **calpain**, mediates limited proteolysis of substrates, such as tubulin, and is involved in cytoskeletal remodeling and signal transduction (Lebart and Benyamin, 2006). In our experiment, the E2-induced expression of Arl3 and calpain may reflect a decreased acetylation of tubulin, and an increased flexibility of the microtubular cytoskeleton (Fig. 4). In other studies, E2 induced the gene expression of calpain in serotonergic neurons or in the cardiac tissue *in vivo* (Bethea and Reddy, 2008; Hamilton et al., 2008).

Dynamics of the microtubular skeleton regulate the activity of protein phosphatase 2A (PP2A), which is the main substrate of the **protein phosphatase methylesterase 1** (PPME1) (Lee et al., 1996). Demethylation of the PP2A catalytic domain decreases its activity (Xing et al., 2008); a lower level of PPME1 may refer to a higher activity of PP2A. PP2A is important in the termination of E2-induced signaling,

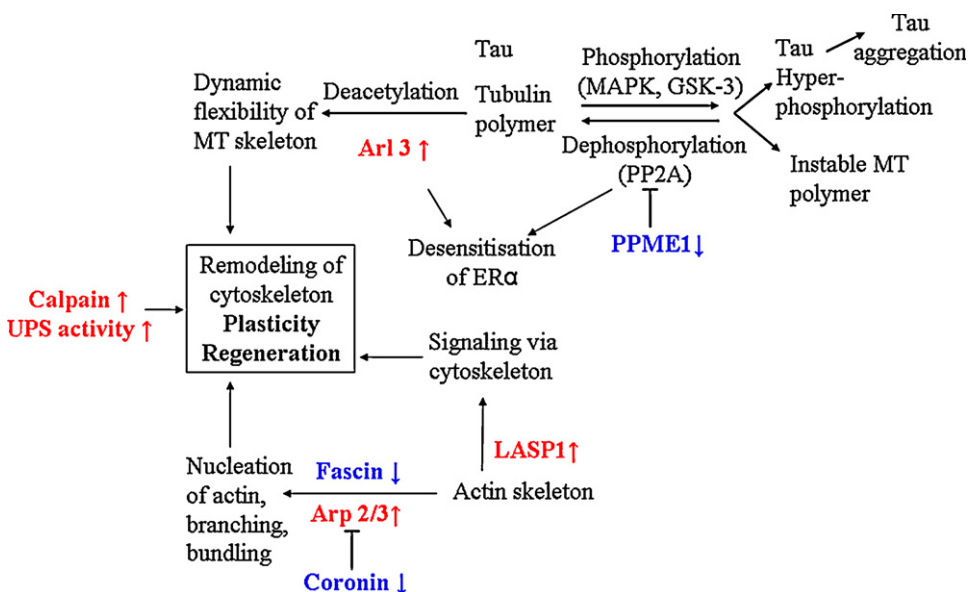


**Figure 4** Schematic illustration of E2-induced cytoskeletal flexibility. E2-induced actin-nucleation (Arp2/3, Coronin), bundling (fascin) and tubulin deacetylation (Arl3) are responsible for improved regeneration and plasticity. Inhibition of PPME1 results in the dephosphorylation of tau. Decreased methylation (PPME1) and acetylation (Arl3) of ER $\alpha$  lead to desensitization to increased E2 concentration. Bold characters depict proteins identified in present study, whereas un-bolded characters depict additional members of the network that were not detected by DIGE/MS.  $\uparrow/\downarrow$ : expression increased/decreased after E2 treatment. Arl3: ADP-ribosylation factor-like 3; MAPK: mitogen activated protein kinase; GSK-3: glycogen synthase kinase 3; PP2A: protein phosphatase 2A; PPME1: protein phosphatase methylesterase 1; MT: microtubule; UPS: ubiquitin–proteasome system; Arp2/3: actin related protein 2/3; and LASP-1: LIM and SH3 domain protein 1.

such as the timing of mitogen activated protein kinase phosphorylation (Belcher et al., 2005). Moreover, PP2A can be in complex with ER $\alpha$ , which *in vitro*, inhibiting E2-induced "non-classical" signaling (Lu et al., 2003). We suggest that the increased activity of PP2A (due to the decreased level of PPME1) results in the inhibition of ER $\alpha$ -E2-induced "non-classical" signaling. In addition, PP2A is one of the main dephosphorylating enzymes of tau, and activation of PP2A through PPME1 inhibition could be an important mechanism by which E2 exerts a protective effect against Alzheimer disease (AD) (Singh et al., 2006). Indeed, it has been reported that decreased activation of PP2A by reduced methylation of PP2A could be responsible for its decreased activation and increased tau hyperphosphorylation (Zhou et al., 2008) (Fig. 4).

In the context of normal cells, it is well accepted that the plasticity of the cytoskeleton and cellular repair is modulated via the activities of actin-associated proteins, and actin itself regulates the highly dynamic structure of postsynaptic sites, especially dendritic spines. **Coronin 1a** and **actin related protein 2/3 complex** (Arp2/3) are actin-binding proteins with altered expression after 24 h E2 treatment. While coronin inhibits actin nucleation and actin-Arp2/3 binding, Arp2/3 increases polymerization, mainly at branch points (Le Clainche et al., 2003). Lower expression of coronin and higher level of Arp2/3 may lead to actin nucleation and branch-formation. Sanchez et al. also found that Arp2/3-dependent control of actin polymerization and branching is very important event in the E2-regulated spine formation (Sanchez et al., 2009). However, expression of the actin-bundling protein **fascin** was decreased by E2 treatment, which could result in actin reorganization and synaptic remodeling (Meller et al., 2008). The expression of the adaptor protein **LIM and SH3 domain protein 1** (LASP-1) also increased after E2 treatment. Protein kinase A-dependent phosphorylation of LASP-1 leads to the redistribution of the protein from the synaptic region to the cytoplasm (Chew et al., 2002; Phillips et al., 2004), hence regulating the E2-induced cytoskeletal reorganization in dendritic spines. E2 was shown to induce actin remodeling and synapse formation also in an Akt- and LIM kinase-dependent manner (Spencer et al., 2008), and it regulates dendritic spine formation and density during the estrous cycle (Woolley and McEwen, 1992). Interestingly, combined E2 and NMDAR activation induced a persistent increase in spine density and silent synapses of cortical neurons, independently from ER $\alpha$  (Srivastava et al., 2008). Regulation of cellular movement by steroids through the actin skeleton was reviewed recently (Giretti and Simoncini, 2008).

#### 4.1.2. Altered glucose utilization and increased antioxidant capacity following E2 treatment

Many of the proteins with altered expression belong to the "Metabolism" group (Table 1). E2 regulation of cellular energetic pathways was evidenced by decreased expression of enzymes of the glycolysis and TCA cycle (**glycerol phosphate dehydrogenase**, **phosphoglycerate kinase**, **pyruvate dehydrogenase (lipoamide) beta**, **citrate synthase**). On the other hand, proteins within the electron transport chain and complex I were increased in expression (**electron transferring flavoprotein**, **NADH dehydrogenase Fe-S protein 8**). That result is contradictory with decreased glycolytic metabolic

activity, suggesting that brain energy consumption was covered from sources other than glycolysis. Although glucose is the major oxidative fuel for brain, fatty acids (FA) can also be utilized for energy production. NMR studies have revealed that FA are oxidized by rodent brain tissue and can directly contribute to up to ~20% of energy consumption (Ebert et al., 2003). The E2 induced utilization of FA, in preference to sugars, is supported by the fact that expression of **glutamate oxaloacetate transaminase-2** (fatty acid-binding protein) increased after E2 treatment. This protein is important not only in glutamate metabolism, but it also facilitates cellular uptake of long-chain FA (Glatz et al., 2001), providing additional data as to regulatory role of E2 in energy utilization.

Metabolic activity regulates the production of free radicals. Enhanced oxidative phosphorylation, and thus increased ATP synthesis via the respiratory chain, requires more oxygen and generates more free radicals, which can damage cells (Singh et al., 2006). The E2-inducible mitochondrial **manganese superoxide dismutase** (MnSOD, SOD2) reduces superoxide anions (Strehlow et al., 2003), while the majority of the mitochondrial peroxides are naturalized by **peroxiredoxins** (PXNs, Kalinina et al., 2008). A portion of the radicals are released into the cytoplasm, where enzymes, such as the **glutathione S-transferase** (GlutST) detoxify the peroxidized macromolecules. In our experiment, the increased level of SOD2, PXN-3 and GlutST indicate that E2 is not only an antioxidant hormone, but induces the synthesis of cytoplasmic and mitochondrial antioxidant proteins (Viña et al., 2005). Confirming our protein expression data, E2 did induce expression of SOD or GlutST in other studies (Bethea and Reddy, 2008; Hamilton et al., 2008).

#### 4.1.3. Estrogen regulates protein metabolism and basal synaptic activity

It is known that increased protein turnover prevents aggregation of misfolded or oxidized proteins. **Aspartyl aminopeptidase** is an important element of the intracellular peptide and protein metabolism, and it is also an amyloid degrading enzyme, which cleaves the amyloid peptide and thereby prevents amyloid plaque formation (Saido, 1998; Iwata et al., 2005). In addition, the low or inadequate activity of the ubiquitin-proteasome system (UPS) also results in the accumulation of damaged proteins. In our model, E2 may increase protein degradation via up-regulation of the **macropain** and aspartyl aminopeptidase expression, preventing aggregation of misfolded or oxidized proteins.

Moreover, UPS and calpain play an important role in the remodeling of the cytoskeleton, axonal growth and synapse formation (Patrick et al., 2003; Patrick, 2006). The presynaptic **deubiquitinating enzyme**, which expression is decreased after E2 treatment, can modulate proteins important in vesicle docking and exocytosis, whereby it regulates the timing of neuronal transmission (Patrick et al., 2003). In addition, decreased amount of **syntaxin binding protein 1** (Munc-18), **vesicular-fusion protein** (NSF), the motor protein **dynein** and the adaptor protein **dynamitin** may refer to an altered (slightly reduced) basal synaptic communication already described at 24 h after E2 treatment (for review, see Kim and Chang, 2006; Rizo and Rosenmund, 2008; Südhof and Rothman, 2009). **Protein phosphatase 3** (calcineurin, CaN) is one of the main neuronal Ca<sup>2+</sup>-dependent phospho-

tases, and its expression is decreased after E2 treatment, supporting previously observed measurements (Zhou et al., 2004). CaN initiates clathrin-dependent endocytosis through dephosphorylation of dynamin (Cousin, 2000), suggesting that E2 may reduce formation of clathrin-coated pits. CaN also activates neuronal nitrogen monoxide synthase (nNOS, Rameau et al., 2003), so decreased levels of CaN after E2 treatment may also result in lower NO production during glutamate transmission (less neurotoxic effect). However, the expression and activity of NOS shows a functional gender difference (Panzica et al., 2006).

In the glutamate metabolic pathway, expression of the mitochondrial **glutamate oxaloacetate transaminase-2 (AAT)** increased, while **glutamate dehydrogenase 1 (GDH)** and **glutamin synthetase (GS)** decreased after E2 treatment. Since AAT and GS are both enzymes responsible for synthesis of glutamate, the opposite changes in their amount after E2 treatment is contradictory. However, in synaptosomes, the predominant route of nitrogen disposal from glutamate is through the AAT reaction, and the 2-oxoglutarate can serve as metabolic fuel for ATP production (Erecińska et al., 1988). Moreover, utilization of glutamate via AAT reaction is accelerated during low-glucose flux. So in parallel with the above described decreased glycolysis, glutamate can be redirected from its neurotransmitter pool via AAT-mediated reaction into the metabolic pool utilized by TCA cycle. However, as turnover of neurotransmitter amino acids is one of the major biosynthetic activities in the brain, we propose that E2-reduced glycolysis decreases the AA pool in the cells, and the increased AAT level reduces the neurotransmitter pool of glutamate. Our data thus suggest a putative mechanism by which E2 acts on AA metabolism and protein turnover, decreasing overall neuronal excitability as a long-term effect. Such a mechanism could lie behind the decreased vulnerability of nerve cells in observed excitotoxic models (Hilton et al., 2006). The E2-induced depletion of glutamatergic transmission could play a role in psychiatric diseases such as depression, suggested by the high number of female depression patients in comparison to male (Bergemann and Riechter-Rössler, 2005). Contrary to this hypothesis, Blutstein et al. (2006) found that E2 increased the gene and protein expression of glutamine synthase in the hippocampus and basal HT of female mice. In their study the amount of E2 was 10 times higher (10 µg instead of 1 µg used in this study), which might explain the difference in the tendency of the expression. According to the hormetic dose–response model (Calabrese and Baldwin, 2003), the low and high dose of E2 might trigger opposite response, in this case the opposite direction of protein expression. Moreover, Li et al. (2007) presumed that mechanisms of action of steroid hormone receptors are particularly a U-shaped or inverted U-shaped response. Finally, Blutstein et al. analyzed homogeneous tissue samples with known estrogen receptor content in their experiment, whereas in our study we analyzed the whole brain extract. Moreover, our hypothesis about decreased synaptic activity is supported by the results of *in vivo* microdialysis study and measurement of tissue concentrations of AAs, showing decreased extracellular AA levels in the striatum and HT following E2 treatment (Fig. 3). Extracellular concentrations of all measured AAs (among them Glu, Gln, Asp, Asn and Gly) were lower following E2 treatment in both areas. In contrast, whole tissue level (intracellular and extracellular content) of AAs did not change nor decrease, and

interestingly the long-term pattern of changes was different in the two areas. In the striatum, where the expressions of the classical ERs are low, both intracellular and extracellular concentrations of Asp, Glu, Gln, GABA and Ser were decreased by E2, while in the ER-rich HT, Asp, Asn, Gln, Arg and Ala were decreased. In the STR, the shift in the tissue concentration of both excitatory (Asp, Glu, Gln) and inhibitory (GABA) AAs can reflect an overall decrease in synaptic activity. The fact that both Glu and Gln decreased not only in the extracellular but also in the tissue AA pool further supports our hypothesis about redirection of glutamate into the metabolic pool. Interestingly, hypothalamic tissue Glu and GABA concentrations did not change, reflecting a regional difference in the effect of estrogen. However, a decreased level of Arg, a precursor of NO synthesis, can occur in parallel with a decreased CaN expression (see above). Nevertheless, dynamic changes in the concentration of AAs can also be observed during physiological processes, e.g. after a change in diet or sleep–awake cycle (Currie et al., 1995; Kékesi et al., 1997). Our data show that E2 can decrease excitatory AA transmission in the hypothalamus and in the striatum, which effect is likely involved in the pathogenesis of many different brain diseases such as neurodegenerative or psychiatric disorders, being protective in a situation of over-excitation but causing an enhancement of depression. However, in combination with other drugs (progestin), estrogen can decrease the incidence of depression (Young et al., 2007).

In conclusion, here we suggest a complex mechanism of E2-induced reorganization of cellular protein networks that leads to increased cytoskeleton flexibility and decreased excitatory processes at least in the hypothalamus and in the striatum, a mechanism that could serve the purposes of neuroprotection and regeneration. At the same time, other alterations in cellular protein networks could enhance psychiatric disorders such as depression and induce psychological and cognitive dysfunctions in puberty via decreased efficiency of synaptic transmission. We hypothesize that E2 adjusts the cellular steady-state condition to one that is more flexible and rapidly responsive. While none of these alterations alone results in large functional changes in the brain, E2-mediated fine tuning of the whole proteome allows cells to be prepared for toxic insults, and also makes them less responsive to external stimuli.

## Role of the funding source

This work was supported by Regional Center of Excellence – Neurobiological Center of Excellence in Southern Hungary (RET-DNK, to G.D.J.).

## Conflict of interest

The work is all original research carried out by the authors. All authors agree with the contents of the manuscript and its submission to the journal. The manuscript is not being considered for publication elsewhere while it is being considered for publication in this journal. Any research in the paper not carried out by the authors is fully acknowledged in the manuscript. All appropriate ethics and other approvals were obtained for the research. The authors have no conflict of interest.

## Acknowledgements

This work was supported by Regional Center of Excellence – Neurobiological Center of Excellence in Southern Hungary (RET-DNK, to G.D.J.) and by the Deutsche Forschungsgemeinschaft through the DFG Research Center for Molecular Physiology of the Brain (CMPB). We thank Gábor Mórotz for the assistance in immunohistochemical experiments. We are grateful to Péter Batáry, Erin Butler, András Czurkó, Zsolt Datki, József Kardos, Cathy Ludwig and István Merchenthaler for helpful discussion.

## References

- Alban, A., David, S.O., Bjorkesten, L., Andersson, C., Sloge, E., Lewis, S., Currie, I., 2003. A novel experimental design for comparative two-dimensional gel analysis: two-dimensional difference gel electrophoresis incorporating a pooled internal standard. *Proteomics* 3, 36–44.
- Behl, C., 2002. Oestrogen as a neuroprotective hormone. *Nat. Rev. Neurosci.* 3, 433–442.
- Belcher, S.M., Le, H.H., Spurling, L., Wong, J.K., 2005. Rapid estrogenic regulation of extracellular signal-regulated kinase 1/2 signaling in cerebellar granule cells involves a G protein- and protein kinase A-dependent mechanism and intracellular activation of protein phosphatase 2A. *Endocrinology* 146, 5397–5406.
- Bergemann, N., Riechter-Rössler, A., 2005. Estrogen Effects in Psychiatric Disorders. Springer-Verlag, Wien, Austria.
- Bethea, C.L., Reddy, A.P., 2008. Effect of ovarian hormones on survival genes in laser captured serotonin neurons from macaques. *J. Neurochem.* 105, 1129–1143.
- Black, M.M., Baas, P.W., Humphries, S., 1989. Dynamics of alpha-tubulin deacetylation in intact neurons. *J. Neurosci.* 9, 358–368.
- Blake, C.A., Brown, L.M., Duncan, M.W., Hunsucker, S.W., Helmke, S.M., 2005. Estrogen regulation of the rat anterior pituitary gland proteome. *Exp. Biol. Med.* 230, 800–807.
- Blutstein, T., Devidze, N., Choleris, E., Jasnow, A.M., Pfaff, D.W., Mong, J.A., 2006. Oestradiol up-regulates glutamine synthetase mRNA and protein expression in the HT and hippocampus: implications for a role of hormonally responsive glia in amino acid neurotransmission. *J. Neuroendocrinol.* 18, 692–702.
- Brann, D.W., Dhandapani, K., Wakade, C., Mahesh, V.B., Khan, M.M., 2007. Neurotrophic and neuroprotective actions of estrogen: basic mechanisms and clinical implications. *Steroids* 72, 381–405.
- Calabrese, E.J., Baldwin, L.A., 2003. The hormetic dose–response model is more common than the threshold model in toxicology. *Toxicol. Sci.* 71, 246–250.
- Chew, C.S., Chen, X., Parente Jr., J.A., Tarrer, S., Okamoto, C., Qin, H.Y., 2002. Lasp-1 binds to non-muscle F-actin in vitro and is localized within multiple sites of dynamic actin assembly in vivo. *J. Cell. Sci.* 115, 4787–4799.
- Cousin, M.A., 2000. Synaptic vesicle endocytosis: calcium works overtime in the nerve terminal. *Mol. Neurobiol.* 22, 115–128.
- Currie, P.J., Chang, N., Luo, S., Anderson, G.H., 1995. Microdialysis as a tool to measure dietary and regional effects on the complete profile of extracellular amino acids in the hypothalamus of rats. *Life Sci.* 57, 1911–1923.
- Ebert, D., Haller, R.G., Walton, M.E., 2003. Energy contribution of octanoate to intact rat brain metabolism measured by <sup>13</sup>C nuclear magnetic resonance spectroscopy. *J. Neurosci.* 23, 5928–5935.
- Erecińska, M., Zaleska, M.M., Nissim, I., Nelson, D., Dagani, F., Yudkoff, M., 1988. Glucose and synaptosomal glutamate metabolism: studies with [<sup>15</sup>N]glutamate. *J. Neurochem.* 51, 892–902.
- Garcia-Segura, L.M., Azcoitia, I., DonCarlos, L.L., 2001. Neuroprotection by estradiol. *Prog. Neurobiol.* 63, 29–60.
- Giretti, M.S., Simoncini, T., 2008. Rapid regulatory actions of sex steroids on cell movement through the actin cytoskeleton. *Steroids* 73, 895–900.
- Glatz, J.F., Luiken, J.J., Bonen, A., 2001. Involvement of membrane-associated proteins in the acute regulation of cellular fatty acid uptake. *J. Mol. Neurosci.* 16, 123–132.
- Hamilton, K.L., Lin, L., Wang, Y., Knowlton, A.A., 2008. Effect of ovariectomy on cardiac gene expression: inflammation and changes in SOCS gene expression. *Physiol. Genomics* 32, 254–263.
- Hilton, G.D., Nunez, J.L., Bambrick, L., Thompson, S.M., McCarthy, M.M., 2006. Glutamate-mediated excitotoxicity in neonatal hippocampal neurons is mediated by mGluR-induced release of Ca<sup>++</sup> from intracellular stores and is prevented by estradiol. *Eur. J. Neurosci.* 24, 3008–3016.
- Iwata, N., Higuchi, M., Saido, T.C., 2005. Metabolism of amyloid-beta peptide and Alzheimer's disease. *Pharmacol. Ther.* 108, 129–148.
- Kalinina, E.V., Chernov, N.N., Saprin, A.N., 2008. Involvement of thio-, peroxi-, and glutaredoxins in cellular redox-dependent processes. *Biochemistry (Mosc.)* 73, 1493–1510.
- Kékesi, K.A., Dobolyi, A., Salfay, O., Nyitrai, G., Juhász, G., 1997. Slow wave sleep is accompanied by release of certain amino acids in the thalamus of cats. *Neuroreport* 8, 1183–1186.
- Kim, Y., Chang, S., 2006. Ever-expanding network of dynamin-interacting proteins. *Mol. Neurobiol.* 34, 129–136.
- Kousteni, S., Bellido, T., Plotkin, L.I., O'Brien, C.A., Bodenner, D.L., Han, L., Han, K., DiGregorio, G.B., Katzenellenbogen, J.A., Katzenellenbogen, B.S., Roberson, P.K., Weinstein, R.S., Jilka, R.L., Manolagas, S.C., 2001. Nongenotropic, sex-nonspecific signaling through the estrogen or androgen receptors: dissociation from transcriptional activity. *Cell* 104, 719–730.
- Le Clainche, C., Pantaloni, D., Carlier, M.F., 2003. ATP hydrolysis on actin-related protein 2/3 complex causes debranching of dendritic actin arrays. *Proc. Natl. Acad. Sci. U.S.A.* 100, 6337–6342.
- Lebart, M.C., Benyamin, Y., 2006. Calpain involvement in the remodeling of cytoskeletal anchorage complexes. *FEBS J.* 273, 3415–3426.
- Lee, J., Chen, Y., Tolstykh, T.S., Stock, J., 1996. A specific protein carboxyl methyltransferase that demethylates phosphoprotein phosphatase 2A in bovine brain. *Proc. Natl. Acad. Sci. U.S.A.* 93, 6043–6047.
- Li, L., Andersen, M.E., Heber, S., Zhang, Q., 2007. Non-monotonic dose–response relationship in steroid hormone receptor-mediated gene expression. *J. Mol. Endocrinol.* 38, 569–585.
- Lu, Q., Surks, H.K., Ebling, H., Baur, W.E., Brown, D., Pallas, D.C., Karas, R.H., 2003. Regulation of estrogen receptor alpha-mediated transcription by a direct interaction with protein phosphatase 2A. *J. Biol. Chem.* 278, 4639–4645.
- Manthey, D., Behl, C., 2006. From structural biochemistry to expression profiling: neuroprotective activities of estrogen. *Neuroscience* 138, 845–850.
- Meller, R., Thompson, S.J., Lusardi, T.A., Ordonez, A.N., Ashley, M.D., Jessick, V., Wang, W., Torrey, D.J., Henshall, D.C., Gafken, P.R., Saugstad, J.A., Xiong, Z.G., Simon, R.P., 2008. Ubiquitin proteasome-mediated synaptic reorganization: a novel mechanism underlying rapid ischemic tolerance. *J. Neurosci.* 28, 50–59.
- Merchenthaler, I., Dellovade, T.L., Shughrue, P.J., 2003. Neuroprotection by estrogen in animal models of global and focal ischemia. *Ann. N. Y. Acad. Sci.* 1007, 89–100.
- Merchenthaler, I., Lane, M.V., Numan, S., Dellovade, T.L., 2004. Distribution of estrogen receptor alpha and beta in the mouse central nervous system: in vivo autoradiographic and immunocytochemical analyses. *J. Comp. Neurol.* 473, 270–291.
- Mitra, S.W., Hoskin, E., Yudkovitz, J., Pear, L., Wilkinson, H.A., Hayashi, S., Pfaff, D.W., Ogawa, S., Rohrer, S.P., Schaeffer, J.M., McEwen, B.S., Alves, S.E., 2003. Immunolocalization of

- estrogen receptor beta in the mouse brain: comparison with estrogen receptor alpha. *Endocrinology* 144, 2055–2067.
- Moosmann, B., Behl, C., 1999. The antioxidant neuroprotective effects of estrogens and phenolic compounds are independent from their estrogenic properties. *Proc. Natl. Acad. Sci. U.S.A.* 96, 8867–8872.
- Nilsen, J., Irwin, R.W., Gallaher, T.K., Brinton, R.D., 2007. Estradiol in vivo regulation of brain mitochondrial proteome. *J. Neurosci.* 27, 14069–14077.
- Panzica, G.C., Viglietti-Panzica, C., Sica, M., Gotti, S., Martini, M., Pinos, H., Carrillo, B., Collado, P., 2006. Effects of gonadal hormones on central nitric oxide producing systems. *Neuroscience* 138, 987–995.
- Patrick, G.N., 2006. Synapse formation and plasticity: recent insights from the perspective of the ubiquitin–proteasome system. *Curr. Opin. Neurobiol.* 16, 90–94.
- Patrick, G.N., Bingol, B., Weld, H.A., Schuman, E.M., 2003. Ubiquitin-mediated proteasome activity is required for agonist-induced endocytosis of GluRs. *Curr. Biol.* 13, 2073–2081.
- Paxinos, G., Franklin, K.B.J., 2001. *The Mouse Brain in Stereotaxic Coordinates*. Academic Press, San Diego, California, USA.
- Phillips, G.R., Anderson, T.R., Florens, L., Gudas, C., Magda, G., Yates, J.R., Colman, D.R., 2004. Actin-binding proteins in a post-synaptic preparation: Lasp-1 is a component of central nervous system synapses and dendritic spines. *J. Neurosci. Res.* 78, 38–48.
- Prokai, L., Prokai-Tatrai, K., Perjesi, P., Zharikova, A.D., Perez, E.J., Liu, R., Simpkins, J.W., 2003. Quinol-based cyclic antioxidant mechanism in estrogen neuroprotection. *Proc. Natl. Acad. Sci. U.S.A.* 100, 11741–11746.
- Rameau, G.A., Chiu, L.Y., Ziff, E.B., 2003. NMDA receptor regulation of nNOS phosphorylation and induction of neuron death. *Neurobiol. Aging* 24, 1123–1133.
- Revankar, C.M., Cimino, D.F., Sklar, L.A., Arterburn, J.B., Prossnitz, E.R., 2005. A transmembrane intracellular estrogen receptor mediates rapid cell signaling. *Science* 307, 1625–1630.
- Rizo, J., Rosenmund, C., 2008. Synaptic vesicle fusion. *Nat. Struct. Mol. Biol.* 15, 665–674.
- Saido, T.C., 1998. Alzheimer's disease as proteolytic disorders: anabolism and catabolism of beta-amyloid. *Neurobiol. Aging* 19, 69–75.
- Sanchez, A.M., Flamini, M.I., Fu, X.D., Mannella, P., Giretti, M.S., Goglia, L., Genazzani, A.R., Simoncini, T., 2009. Rapid signaling of estrogen to WAVE1 and moesin controls neuronal spine formation via the actin cytoskeleton. *Mol. Endocrinol.* 23, 1193–1202.
- Shevchenko, A., Wilm, M., Vorm, O., Mann, M., 1996. Mass spectrometric sequencing of proteins silver-stained polyacrylamide gels. *Anal. Chem.* 68, 850–858.
- Singh, M., Dykens, J.A., Simpkins, J.W., 2006. Novel mechanisms for estrogen-induced neuroprotection. *Exp. Biol. Med.* 231, 514–521.
- Spencer, J.L., Waters, E.M., Milner, T.A., McEwen, B.S., 2008. Estrous cycle regulates activation of hippocampal Akt, LIM kinase, and neurotrophin receptors in C57BL/6 mice. *Neuroscience* 155, 1106–1119.
- Srivastava, D.P., Woolfrey, K.M., Jones, K.A., Shum, C.Y., Lash, L.L., Swanson, G.T., Penzes, P., 2008. Rapid enhancement of two-step wiring plasticity by estrogen and NMDA receptor activity. *Proc. Natl. Acad. Sci. U.S.A.* 105, 14650–14655.
- Strehlow, K., Rotter, S., Wassmann, S., Adam, O., Grohé, C., Laufs, K., Böhm, M., Nickenig, G., 2003. Modulation of antioxidant enzyme expression and function by estrogen. *Circ. Res.* 93, 170–177.
- Südhof, T., Rothman, J.E., 2009. Membrane fusion: grappling with SNARE and SM proteins. *Science* 323, 474–477.
- Szegő, É.M., Barabás, K., Balog, J., Szilágyi, N., Korach, K.S., Juhász, G., Ábrahám, I.M., 2006. Estrogen induces estrogen receptor  $\alpha$  dependent CREB phosphorylation via MAPK pathway in basal forebrain cholinergic neurons in vivo. *J. Neurosci.* 26, 4104–4110.
- Viña, J., Borrás, C., Gambini, J., Sastre, J., Pallardó, F.V., 2005. Why females live longer than males? Importance of the upregulation of longevity-associated genes by oestrogenic compounds. *FEBS Lett.* 579, 2541–2545.
- Wang, J., Cheng, C.M., Zhou, J., Smith, A., Weickert, C.S., Perlman, W.R., Becker, K.G., Powell, D., Bondy, C.A., 2004. Estradiol alters transcription factor gene expression in primate prefrontal cortex. *J. Neurosci. Res.* 76, 306–314.
- Woolley, C.S., McEwen, B.S., 1992. Estradiol mediates fluctuation in hippocampal synapse density during the estrous cycle in the adult rat. *J. Neurosci.* 12, 2549–2554.
- Xing, Y., Li, Z., Chen, Y., Stock, J.B., Jeffrey, P.D., Shi, Y., 2008. Structural mechanism of demethylation and inactivation of protein phosphatase 2A. *Cell* 133, 154–163.
- Young, E.A., Kornstein, S.G., Harvey, A.T., Wisniewski, S.R., Barkin, J., Fava, M., Trivedi, M.H., Rush, A.J., 2007. Influences of hormone-based contraception on depressive symptoms in premenopausal women with major depression. *Psychoneuroendocrinology* 32, 843–853.
- Zhou, J., Pandey, S.C., Cohen, R.S., 2004. Estrogen decreases levels of calcineurin in rat amygdala and hippocampus. *Neuroreport* 15, 2437–2440.
- Zhou, L., Lehan, N., Wehrenberg, U., Disteldorf, E., von Lossow, R., Mares, U., Jarry, H., Rune, G.M., 2007. Neuroprotection by estradiol: a role of aromatase against spine synapse loss after blockade of GABA(A) receptors. *Exp. Neurol.* 203, 72–81.
- Zhou, X.W., Gustafsson, J.A., Tanila, H., Bjorkdahl, C., Liu, R., Winblad, B., Pei, J.J., 2008. Tau hyperphosphorylation correlates with reduced methylation of protein phosphatase 2A. *Neurobiol. Dis.* 31, 386–394.